International Conference
Nuclear Energy for New Europe 2004
Portorož • Slovenia • September 6-9

port2004@ijs.si
www.drustvo-js.si/port2004
+386 1 588 5247, fax +386 1 561 2276
PORT2004, Nuclear Society of Slovenia, Jamova 39, SI-1000 Ljubljana, Slovenia

Simulation of Containment Atmosphere Stratification Experiment Using Local Instantaneous Description

Miroslav Babić, Ivo Kljenak
Reactor Engineering Division
"Jožef Stefan" Institute
Jamova 39, SI-1000 Ljubljana, Slovenia
miroslav.babic@ijs.si, ivo.kljenak@ijs.si

ABSTRACT

An experiment on mixing and stratification in the atmosphere of a nuclear power plant containment at accident conditions was simulated with the CFD code CFX4.4. The original experiment was performed in the TOSQAN experimental facility. Simulated non-homogeneous temperature, species concentration and velocity fields are compared to experimental results.

1 INTRODUCTION

An important topic in the field of nuclear safety is hydrogen behavior in nuclear power plant containment at accident conditions. One of the main issues is to predict whether, due to atmosphere mixing and stratification, the local hydrogen concentration in certain parts of the containment will exceed flammability limits. Lately, many investigations about the possible application of so-called Computational Fluid Dynamics (CFD) codes for this purpose have been started [1-5]. CFD codes solve the transport mass, momentum and energy equations when a fluid system is modeled using local instantaneous description.

These investigations are complemented by adequate experiments. Recently, the following integral experimental facilities have been set up:

- TOSQAN, at the Institut de Radioprotection et de Sureté Nucléaire in Saclay (France),
- MISTRA, at the Commissariat à l' Energie Atomique in Saclay (France),
- ThAI, at Becker Technologies GmbH in Eschborn (Germany).

In contrast to older experimental facilities which were used to investigate containment phenomena at accident conditions, the new facilities are equiped with instrumentation which allows measurement of local temperature, species concentration and velocities. Thus, the non-homogeneous structure and the flow patterns of the containment atmosphere may be observed, which enables a better understanding of mixing and stratification processes in the containment of an actual nuclear power plant. Besides, local experimental measurements may be used to assess the validity of simulations performed by CFD codes.

In the present work, the CFD code CFX4.4 [6], which is perfectly adequate for the intended purpose, was used to simulate an experiment that was performed in the TOSQAN facility. During the test, steam, air and helium were injected in a cylindrical vessel at various

flow rates, and steam condensed on parts of the vessel walls. Calculated horizontal profiles of temperature, steam and helium concentration, and vertical velocity at different elevations in the vessel are presented and compared to experimental results.

2 EXPERIMENT

2.1 Experimental Facility

The TOSQAN experimental facility [7, 8] is a cylindrical vessel with an internal volume of 7.0 m^3 (Fig. 1). The temperature of the vessel walls may be controlled, so that the walls are divided into a "hot" zone and a "cold" (condensation) zone. Steam and other gases are injected through a vertical tube located at the vessel center-line.

2.2 Experimental Procedure

In the present work, a test performed within Phase 1 of the OECD International Standard Problem on containment thermal-hydraulics was considered [7]. The vessel was initially filled with air. During the test, air, steam and helium were injected intermittently with various mass flow rates. The temperature of the walls was controlled. The sump was drained continuously. Steam condensation occurred only on walls with lower temperature (area: 9.40 m^2). The thermal-hydraulic behavior was determined by the following physical phenomena: gas injection, steam condensation, heat transfer and buoyant flow. During certain phases of the experiment, steady states were reached when the steam condensation rate became equal to the steam injection rate, with all boundary conditions remaining constant.

Three steady states (referred in the present work as 1, 2 and 3), which were obtained with different boundary conditions, were simulated independently. The (measured) parameters of the steady states are provided in Table 1 [8]. The temperatures of the upper and lower non-condensing wall were 122.0 ºC and 123.5 ºC, respectively. The temperature of the condensing wall was 101.8 ºC during steady states 1 and 3, and 107.8ºC during steady state 2.

Table 1. Parameters of steady states during experiment in TOSQAN vessel

	Steady state 1	Steady state 2	Steady state 3
Pressure, bar	2.40	3.01	2.42
Average temp., ºC	113.7	119.7	114.4
Air mass, kg	8.18	8.18	10.0
Initial steam mass, kg	4.37	6.60	Not reported
Helium mass, kg	–	–	0.618
Steam injection rate, g/s	1.11	12.27	0.89

3 INPUT MODEL

3.1 Geometric Model

A two-dimensional axisymmetric model (in cylindrical coordinates) for the code CFX4.4 was developed. The computational domain is a block with 160 cells in the axial (vertical) direction and 30 cells in the radial (horizontal) direction (Fig. 2). There are 4800

cells altogether. The width (radial direction) of each cell depends on the axial location. Thus, cells located within the vessel sump are much narrower than cells located within the condensation region (Fig. 1). The condensation zone extends from z = 2.391 m to z = 4.391 m and includes 67 rows of cells. In the condensation zone, the width of the cells contiguous to the vessel wall is 2.0 cm.

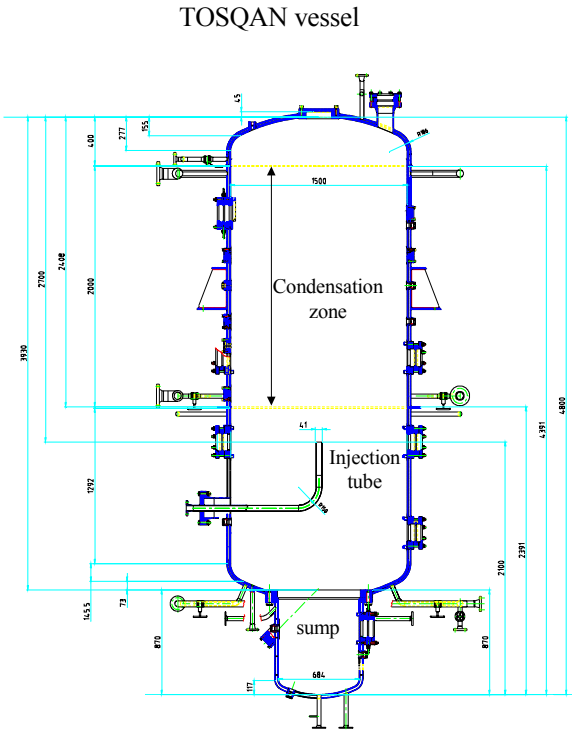

Figure 1. Schematic view of the TOSQAN experimental facility [7].

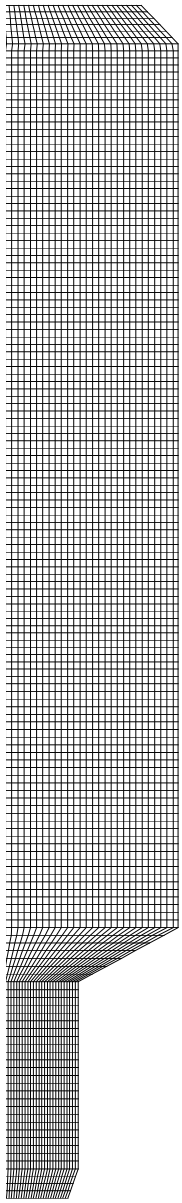

Figure 2. Numerical grid of TOSQAN vessel for CFX code.

3.2 Physical Model

The air-steam and air-steam-helium atmospheres were treated as single-phase gaseous mixtures, which are homogeneous within each computational cell. The following options were prescribed in the CFX "command file":

- compressible flow,
- turbulent flow (k-ε model),
- buoyant flow,
- no-slip condition at the vessel wall.

The default options of the CFX4.4 code, which correspond to these physical models, were applied.

The modeling of condensation is not implemented in most current CFD codes, including CFX. In the present work, steam condensation was modeled as a sink of mass and enthalpy by applying the Uchida correlation [9] that was basically developed for an integral approach. The condensate film on the "cold" wall was not considered. The Uchida correlation is based on experiments on natural convection from relatively small vertical plates and was originally developed to be used for "integral" (volume-averaged) modeling of steam condensation in the presence of non-condensable gases. Basically, the steam condensation rate on a vessel wall with area A is obtained from the expression:

$$M^0 = C_u \, (\rho_{steam}/\rho_{non\text{-}cond})^{0.8} \cdot A \cdot (T - T_{wall}) \, / \, h_{lg} \tag{1}$$

where C_u is an adjustable coefficient, h_{lg} denotes the latent heat of evaporation, and all the physical variables, except T_{wall}, refer to "bulk flow" conditions in the vessel. The corresponding enthalpy sink (enthalpy flow) due to condensation may then be calculated as:

$$H^0 = m^0 \cdot c_p \cdot (T - T_{ref}) \tag{2}$$

where T_{ref} denotes some reference temperature at which the enthalpy is zero. We have decided to use Uchida's correlation, although it is known to be in error when condensing surfaces are tall so that condensate films become thick and create significant thermal resistance, and when steam jets and other sources of forced convection augment natural convection flow [10].

The modeling of condensation was implemented in a user-defined subroutine. Sinks of mass and enthalpy occurred in cells contiguous to the condensing wall. In each cell, the mass sink was calculated from Eq. (1) where the "bulk flow" physical quantities (temperature, steam density, air density) were evaluated at the cell center. For each cell, the area A was calculated as:

$$A = 2\pi \cdot R \cdot \Delta z \tag{3}$$

where R denotes the local vessel radius and Δz the cell height. Similarly, the enthalpy sink was calculated from Eq. (2). The sensible heat flux through vessel walls was computed by the CFX code.

4 RESULTS AND DISCUSSION

Each steady state was simulated separately. For each simulation, the initial pressure and average temperature in the vessel were set to the measured values. The value of the coefficient C_u (Eq. 1) was adjusted to obtain a reasonably good agreement between measured and calculated pressure and average atmosphere temperature during steady states. The same value C_u = 200 W/m^{2}K was used for all three steady states. The initial steam mass fraction was calculated so that the mass of air in the vessel was equal to the sum of the initial and injected masses. In the simulation of steady state 3, the mass of injected helium prior to the steady state was also taken into account. For each steady state, the simulation was run until the condensation rate became equal to the steam injection mass flow rate, and the variations of pressure and average temperature became small enough.

Measured [8] and calculated pressure and average temperatures, obtained with the prescribed value of the coefficient C_u, are presented in Table 2. The differences between experimental and simulated values are relatively small, except perhaps for the pressure during steady state 2 (where the relative difference is still lower than 5%).

Table 2. Measured and calculated pressure and average temperature.

		Steady state 1	Steady state 2	Steady state 3
Pressure, bar	Experiment	2.40	3.01	3.42
	Simulation	2.39	3.15	3.37
Average temperature, ºC	Experiment	113.7	119.7	114.4
	Simulation	113.6	118.5	113.8

Figures 3-12 show the measured and calculated radial profiles of temperature, steam and helium volumetric concentration and vertical velocity during the three steady states at representative vertical positions (elevations). Although the computational domain was only one half of a vertical plane, symmetric results are shown over the entire vessel for comparison with experimental data on both sides of the vessel axis. The uncertainties of temperature, volumetric concentration and velocity measurements are ±1 ºC, up to ± 2.3% and up to ±10 % of the measured value, respectively.

For the temperature profiles, a very good agreement was obtained for steady state 1 (Fig. 3) and steady state 3 (Fig. 9). For steady state 2 (Fig. 6), the simulated temperatures at higher elevations are somewhat underpredicted. In particular, the code did not simulate the high temperature at the vessel center-line above the injection tube.

For the concentration profiles, the simulation replicated the relatively homogeneous atmosphere during steady states 1 and 3 (Figs. 4, 10 and 11). The apparently large discrepancies are due to the scale on the ordinata axis. For steady state 2, where the atmosphere was less homogeneous due to the higher steam injection rate, a good agreement may be observed at the highest and lowest elevation (except in the near-wall region, which was not modeled in detail in the present work). For the intermediate elevation, the code replicated the experimental pattern but with a shift towards higher values.

The vertical velocities were well simulated for steady states 1 and 3 (Figs. 5 and 12) although in the first case, the velocity in the vessel core was a little overpredicted. For steady state 2 (Fig. 8), the code did not simulate the relatively high velocity at the vessel center-line above the injection tube.

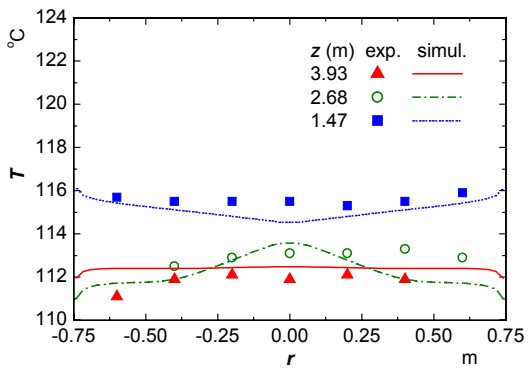

Figure 3. Steady state 1: experimental and simulated temperature radial profiles.

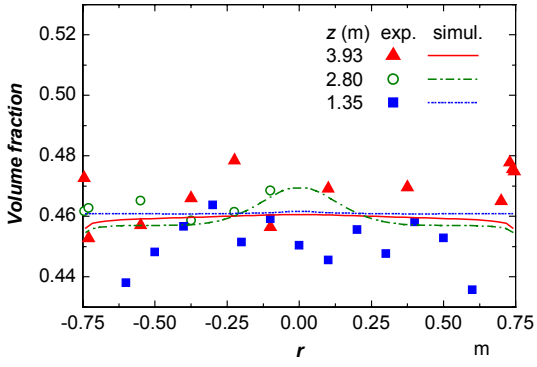

Figure 4. Steady state 1: experimental and simulated radial profiles of steam volume fraction.

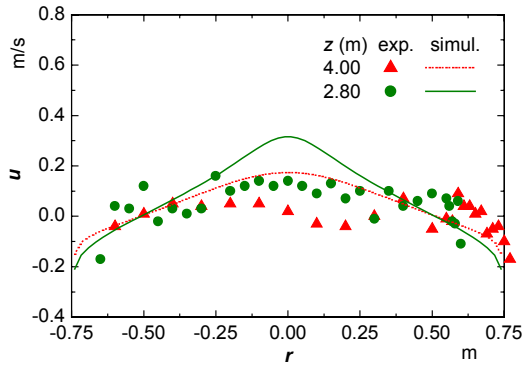

Figure 5. Steady state 1: experimental and simulated radial profiles of vertical velocity.

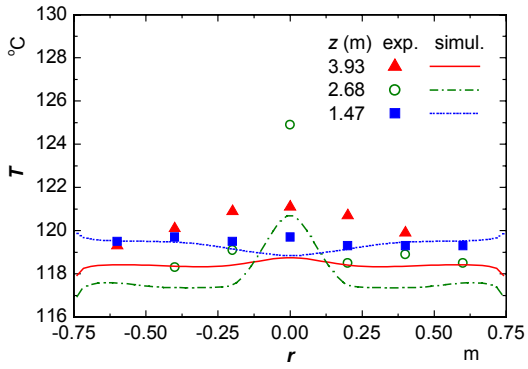

Figure 6. Steady state 2: experimental and simulated temperature radial profiles.

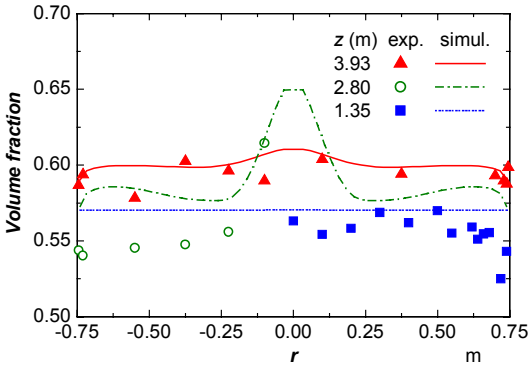

Figure 7. Steady state 2: experimental and simulated radial profiles of steam volume fraction.

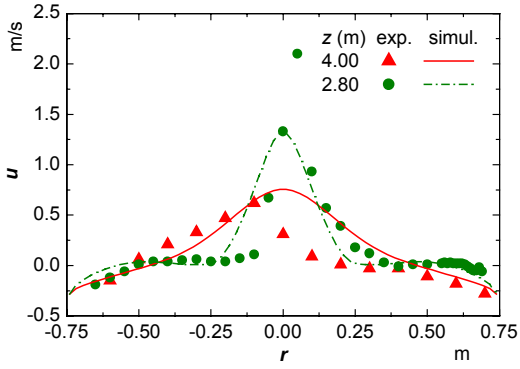

Figure 8. Steady state 2: experimental and simulated radial profiles of vertical velocity.

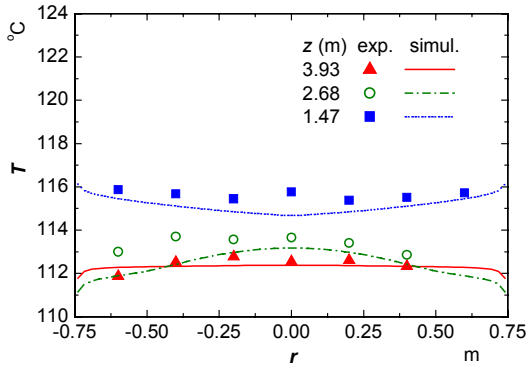

Figure 9. Steady state 3: experimental and simulated temperature radial profiles.

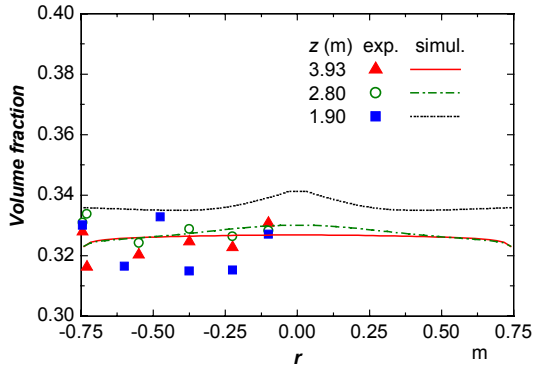

Figure 10. Steady state 3: experimental and simulated radial profiles of steam volume fraction.

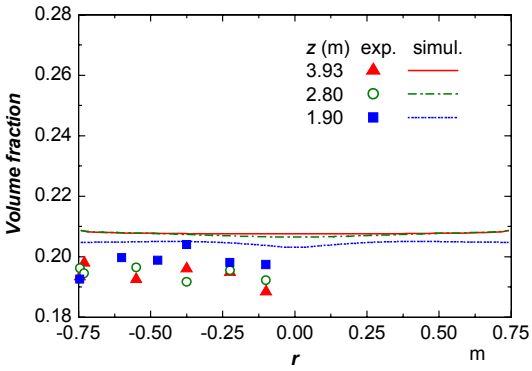

Figure 11. Steady state 3: experimental and simulated radial profiles of helium volume fraction.

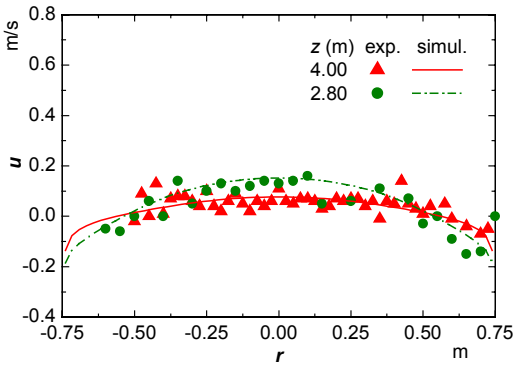

Figure 12. Steady state 3: experimental and simulated radial profiles of vertical velocity.

Figures 13-16 illustrate the steam and helium (for steady state 3) simulated concentration patterns in the vessel. On Fig. 14, the influence of the higher steam injection rate may be observed. Figure 16 shows that, during steady state 3, helium is almost homogeneously distributed in the vessel (except for a small region near the injection tube).

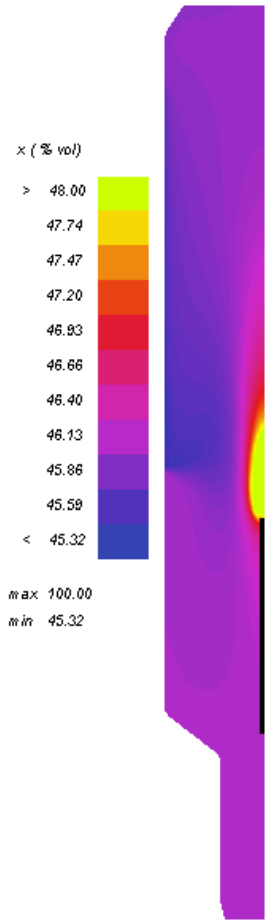

Figure 13. Steady state 1: steam volumetric concentration.

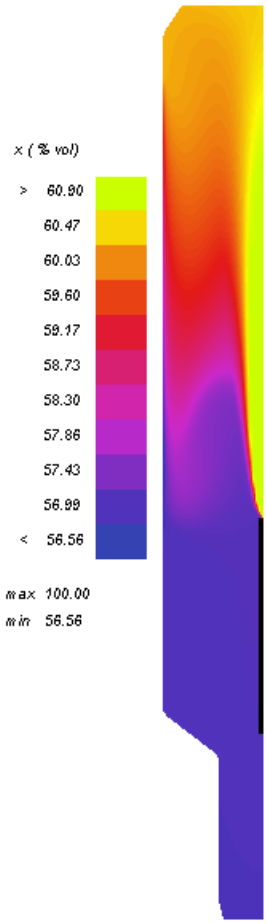

Figure 14. Steady state 2: steam volumetric concentration.

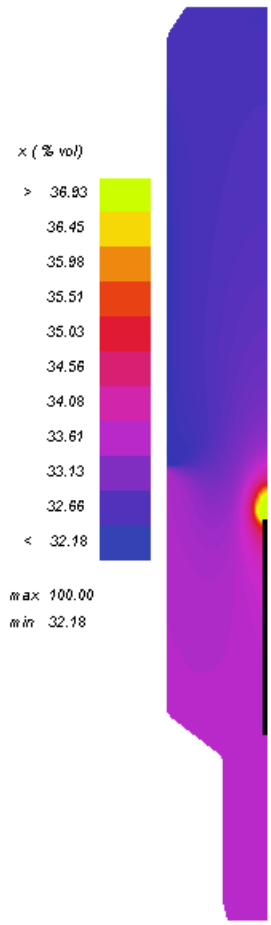

Figure 15. Steady state 3: steam volumetric concentration.

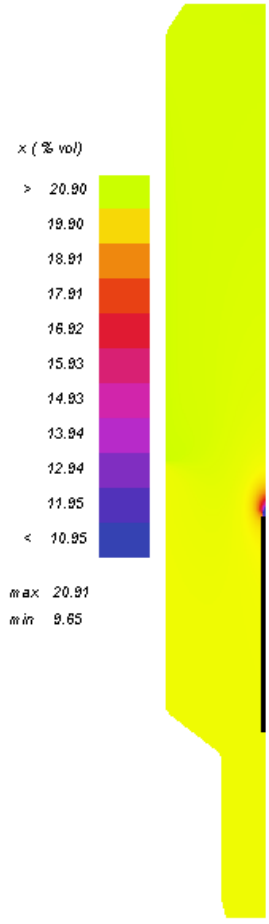

Figure 16. Steady state 3: helium volumetric concentration.

5 CONCLUSIONS

An experiment on containment atmosphere stratification at accident conditions, performed in the TOSQAN experimental facility, was simulated with the CFD code CFX4.4. A two-dimensional axisymmetric model was developed, and steam condensation was modeled by implementing an integral correlation in the CFD code. Despite some discrepancies, the agreement between experimental and calculated results shows that the proposed approach is adequate and could be applied to similar simulations.

ACKNOWLEDGMENTS

The research presented in this work was performed within the research project J2-6614 (contract no. 3311-04-8226614) financed by the Ministry for Education, Science and Sports of the Republic of Slovenia.

The Jozef Stefan Institute is a member of the Severe Accident Research Network of Excellence (SARNET) within the 6th EU Framework Programme. The benefit from European Comission RTD Programme for research is acknowledged.

REFERENCES

[1] B.L. Smith, M. Milelli, S. Shepel, “Aspects of nuclear reactor simulation requiring the use of advanced CFD models”, IAEA-OECD Meeting on Use of CFD Codes for Safety Analysis of Reactor Systems including Containment, Pisa, Italy, 2002.

[2] J.A. Lycklama à Nijeholt, J. Hart, “CFD simulation of thermal-hydraulics in the PHEBUS FP containment vessel”, Proc. 8th Int.Conf. Nuclear Engineering ICONE8, Baltimore, USA, 2000.

[3] J.M. Martin-Valdepenas, M.A. Jimenez, “CFD analyses of hydrogen risk within PWR containments”, IAEA-OECD Meeting on Use of CFD Codes for Safety Analysis of Reactor Systems including Containment, Pisa, Italy, 2002.

[4] A. Rastogi, “CFD application to reactor safety problems with complex flow regimes”, IAEA-OECD Meeting on Use of CFD Codes for Safety Analysis of Reactor Systems including Containment, Pisa, Italy, 2002.

[5] N.B. Siccama, M. Houkema, E.M.J. Komen, “CFD analyses of steam and hydrogen distribution in a nuclear power plant”, IAEA-OECD Meeting on Use of CFD Codes for Safety Analysis of Reactor Systems including Containment, Pisa, Italy, 2002.

[6] AEA TECHNOLOGY plc, CFX-4.3: Solver Manual, Harwell, United Kingdom, 1999.

[7] P. Cornet, J. Malet, E. Porcheron, TOSQAN Experimental Results of the Air-Steam Phase, OECD Int. Stand. Probl. Containment Thermal-Hydraulics ISP-47, IRSN, Saclay, France, 2002.

[8] Ph.Brun, P.Cornet, J.Malet, B.Menet, E.Porcheron, J.Vendel, M.Caron-Charles, J.J.Quillico, H.Paillere, E.Studer, Specification of Int. Stand. Prob. Containment Thermal-Hydraulics ISP-47, Step 1: TOSQAN–MISTRA, IRSN and CEA, Saclay, France, 2002.

[9] T.L. George, A. Singh, “Separate Effects Tests for GOTHIC Condensation and Evaporative Heat Transfer Models”, *Nuclear Engng Design* **166**, 1996, pp. 403-411.

[10] P.F. Peterson, “Theoretical Basis for the Uchida Correlation for Condensation in Reactor Containments”, *Nuclear Engng Design* **162**, 1996, pp. 301-306.